Ultrasonics - Sonochemistry 70 (2021) 105315

Contents lists available at ScienceDirect

Ultrasonics - Sonochemistry

journal homepage: www.elsevier.com/locate/ultson

Characterization of transient cavitation activity during sonochemical modification of magnesium particles

Nadzeya Brezhneva[a,b], Nikolai V. Dezhkunov[c], Sviatlana A. Ulasevich[a], Ekaterina V. Skorb[a,*]

[a] Infochemistry Scientific Center of ITMO University, Lomonosova str. 9, Saint Petersburg 191002, Russia
[b] Belarusian State University, Leningradskaya str. 14, Minsk 220030, Belarus
[c] Belarusian State University of Informatics and Radioelectronics, P. Brovki str. 10, Minsk 220013, Belarus

ARTICLE INFO

Keywords:
Sonochemistry
Transient cavitation
Cavitation bubbles
Magnesium nanostructuring
Magnesium hydroxide
Hydrogen storage

ABSTRACT

Investigation of the cavitation activity during ultrasonic treatment of magnesium particles during nanostructuring has been performed. Cavitation activity is recorded in the continuous mode after switching the ultrasound on with the use of ICA-5DM cavitometer. It has been demonstrated that this characteristic of the cavitation zone may be varied in a wide range of constant output parameters of the generator. The speed and nature of the cavitation activity alteration depended on the concentration of Mg particles in the suspension and the properties of the medium in which the sonochemical treatment has been performed. Three stages of the cavitation area evolution can be distinguished: 1 – the initial increase in cavitation activity, 2 – reaching a maximum with a subsequent decrease, and 3 – reaching the plateau (or the repeated cycles with feedback loops of enlargement/reduction of the cavitation activity).

The ultrasonically treated magnesium particles have been characterized by scanning electron microscopy, X-ray diffraction analysis and thermal analysis. Depending on the nature of the dispersed medium the particles can be characterized by the presence of magnesium hydroxide (brucite) and magnesium hydride. It is possible to reach the incorporation of magnesium hydride in the magnesium hydroxide/magnesium matrix by varying the conditions of ultrasonic treatment (duration of treatment, amplitude, dispersed medium *etc.*). The influence of the magnesium reactivity is also confirmed by the measurements of cavitation activity in organic dispersed media (ethanol, ethylene glycol) and their aqueous mixtures.

1. Introduction

Nowadays the use of ultrasound provides the new possibilities in the synthesis of novel nanomaterials, structuring the surface of the solids for creating materials with the desired properties [1–4]. Ultrasonic cavitation can be regarded as an effective mechanism of the local concentration of relatively low energy of the acoustic field in the small volumes, results in the formation of the areas with high energy density [5,6]. In general, cavitation can be divided into non-inertial (stable) and inertial (transient) cavitation [7]. Stable bubbles pulsate with relatively low amplitudes and can be considered as low-energy bubbles. Strong sonochemical effects are normally caused by transient bubbles, which collapse and produce extreme conditions with local areas of high temperatures and pressures [6,7]. Those bubbles generate shock waves, microjets and chemically active species, such as hydroxyl radicals. Transient cavitation is a key factor in the processes of ultrasonic cleaning [8,9] dispersion of solids, materials surfaces nanostructuring [10–15]. Transient bubbles can be considered as the microcontainers with free radicals and ions – appropriate species for synthesis of nanostructures and modification of solids [10].

Sonochemical activation of metals surfaces leads to the improvement of the materials properties in comparison with non-treated initial ones. Transient cavitation is related with the dynamics of the collapse and in the case of the sonochemical treatment of metals and alloys can be accompanied by different processes – *e.g.* formation of the oxide/hydroxide surface layer in the oxidation media, reverse process of the reduction of the components in the reducing media (for example, in the presence of radical scavengers), recrystallization processes, amorphization or solidification *etc*. [16] Ultrasound can be served as a convenient tool for improvement of materials properties for various applications – electrocatalytic water splitting [13], improvement of biocompatibility [15], porous matrices for encapsulation of bioactive molecules, corrosion inhibitors [11,14] *etc*. For instance, ultrasonic treatment of titanium in aqueous alkaline solutions leads to the

* Corresponding author.
E-mail address: skorb@itmo.ru (E.V. Skorb).

https://doi.org/10.1016/j.ultsonch.2020.105315
Received 27 February 2020; Received in revised form 18 August 2020; Accepted 18 August 2020
Available online 26 August 2020

formation of porous layer based on titanium dioxide, improving biocompatibility compared to the initial, non-treated material [12]. In addition, application of the ultrasound can also facilitate hydrogen production in the process of laser ablation of reactive metals (*e.g.* aluminium, magnesium and their alloys) [17].

Sonochemical treatment of magnesium in various solvents (water, ethanol) with additives towards investigation of magnesium hydroxide (brucite) formation was performed by Baidukova et al. [18]. Magnesium hydroxide, due to its specific properties, has found applications in many fields. It is widely used in fire-resistant composite materials due to its ability to decompose endothermally with the release of water at high temperatures without the formation of toxic or corrosive substances, as well as an acid waste neutralizer in the paper industry and in the field of environmental protection. In addition, nanosized MgO products are usually formed as a result of thermal decomposition of $Mg(OH)_2$ precursors [19]. Thus, it was shown that the use of ultrasound is a convenient way to obtain nanosized crystalline magnesium hydroxide [18]. Also, the possibility of the formation of hybrid capsules with a polypyrrole/magnesium interface formed during the polymerization of a monomer (pyrrole) presented in the treated medium was shown by E. V. Skorb et al. [20].

Recently, the possibility of the sonochemically treated Mg for the reactive hard templating has been demonstrated [10]. In last decades, the perspective of its use as hydrogen storage material has been shown [21,22]. Sonochemical treatment provides possibility of the low-energy hydrides formation, particularly, in the case of magnesium particles treatment. Particularly, Baidukova et al. demonstrated the possibility to form low-energy hydrides in a porous magnesium-magnesium hydroxide matrix by means of the sonochemical treatment of magnesium particles in aqueous suspensions [10].

Since a significant amount of hydrogen in the form of bubbles is released during the contact of magnesium with water, this phenomenon can affect cavitation and its role in surface and structural modification. Until now, no attention has been paid to this, although it is clear that knowledge of the cavitation behavior is necessary to select the optimal treatment regime.

In this regard, the aim of our research is to study the evolution of cavitation activity during ultrasonic treatment of magnesium particles in suspensions. In addition, characterization of the sonochemically modified Mg particles has been performed.

2. Experimental

2.1. Experimental setup

In the work, micrometer-sized magnesium particles –325 mesh, 99.8%, Alfa Aesar), ethanol (absolute, Sigma Aldrich), ethylene glycol (99%, Carl Roth), were used as received and organic:water solutions at different volume ratios (in percent, %) – (20:80, 50:50 and 80:20) were prepared. Ultrasound generator (UZG 55–22, 20 kHz, 100 W) was produced in Belarusian State University of Informatics and Radioelectronics. In our experiments, we used the fixed volume of the suspensions, it comprised 100 mL, for preparing the suspensions of the particles with their concentrations 0.0005 g/mL, 0.001 g/mL, 0.003 g/mL, 0.007 g/mL, 0.010 g/mL we used 0.05 g, 0.1 g, 0.3 g, 0.7 g, and 1.0 g of Mg powder, respectively. The experiment was performed in the following manner – we added the amount of particles we needed (0.05 g, 0.1 g, 0.3, 0.7 or 1.0 g) to prepare the suspension with the appropriate concentration of particles (0.0005, 0.001, 0.003, 0.007, and 0.010 g/mL, respectively), stirred the suspension for 10 s and after that switched the ultrasound on.

Titanium sonotrode was used as a source of ultrasonic vibrations at vibration amplitude of 14 μm as measured by vibrometer VM1-5 (Minsk, Belarus), input power – 65 W. The sonotrode was made in the form of a truncated cone with a disk on the immersed end. The diameter of the disc was 12 mm, the thickness comprised 2 mm.

Cavitometer ICA-5D (BSUIR, Belarus) was used for transient cavitation activity recording. The physical principle of operation of this device is based on a spectral analysis of cavitation noise, *i.e.* acoustic signal generated by the cavitation area [7,23]. The sensor of the device is a cylindrical waveguide with a diameter of 3 mm. A piezoelectric plate is installed on one end of sensor. Through the waveguide, the acoustic signal from cavitation zone is transmitted to the piezoplate, where it is converted into an electric one. The output of the device is formed as the integral of wideband component of the cavitation in the frequency range from 10 kHz to 10 MHz.

The cavitometer allows measuring (in arbitrary units) total activity of cavitation and the contribution of collapsing bubbles, *i.e.* activity of transient cavitation. The device is equipped with a software that allows recording data of the cavitation activity and simultaneously display them on a computer monitor in a real time. The measurement results are saved in the form of graphs and tables as separate files automatically based on the storage algorithm selected by the operator. Range switching during data recording can be performed automatically or manually. The duration of the experiment, *i.e.* the duration of registration can be chosen by the operator.

Recordings were performed for two different positions of the sensor – under the sonotrode tip at a distance of 1 cm below the sonotrode and near the sonotrode tip at a distance of 2 cm from its center. The schematic and photo illustrations of the setup are presented in Fig. 1. In our experiments, we checked the temperature of the electrolyte at the beginning and at the end of the experiment. The initial temperature of each electrolyte was 20° ± 1°C. The sonication was conducted at constant cooling of the electrolyte. At the end of the sonication, the temperature of the suspensions contained ethanol or water increased up to 3° ± 1°C and 4° ± 1°C for ethanol and water content, respectively. The electrolyte with ethylene glycol was heated after the sonication up to 8° ± 1°C.

The suspensions were sonicated for 15 min, and the particles were filtered using convenient paper filter (pore size is 2–3 μm) under vacuum conditions. Then the particles were washed with water, filtered again, and then dried at 100 °C until the constant mass of the sample. After sonication of the particles in non-aqueous media, the particles were separated from the electrolyte using the same paper filter, washed with ethanol, and dried at the same conditions as described above.

First, experiments to study the cavitation activity in magnesium contained suspensions were performed in distilled water. An appropriate amount of magnesium powder (0.05 g, 0.1 g, 0.3 g, 0.7 g or 1.0 g) was added in water and afterwards, the cavitation activity was immediately recorded. The duration of 15 min for the ultrasonic treatment was chosen as the optimal time for the cavitation analysis. The longer duration of treatment led to a non-reproducibility of measurements taking into account the maximum term of ultrasound (US) generator exploitation in the continuous mode and heating of the suspension. The shorter treatment of magnesium contained suspension did not provide the formation of hydride phase. All measurements were performed 3 times for controlling the reproducibility of the measurements. The presented data are the average curves of three independent experiments (Fig. S1).

2.2. Particles characterization

2.2.1. Scanning electron microscopy

The morphology of obtained particles was evaluated using a Tescan Vega 3 scanning electron microscope (Czech Republic) in the secondary electron detection mode with an operating voltage of 5 kV. Before the operating procedure the samples were sputtered with carbon in order to provide a better conductivity of the sample.

2.2.2. X-ray diffraction analysis

The phase composition was determined using Empyrean powder diffractometer (PANalytical, Netherlands) with CuKα radiation

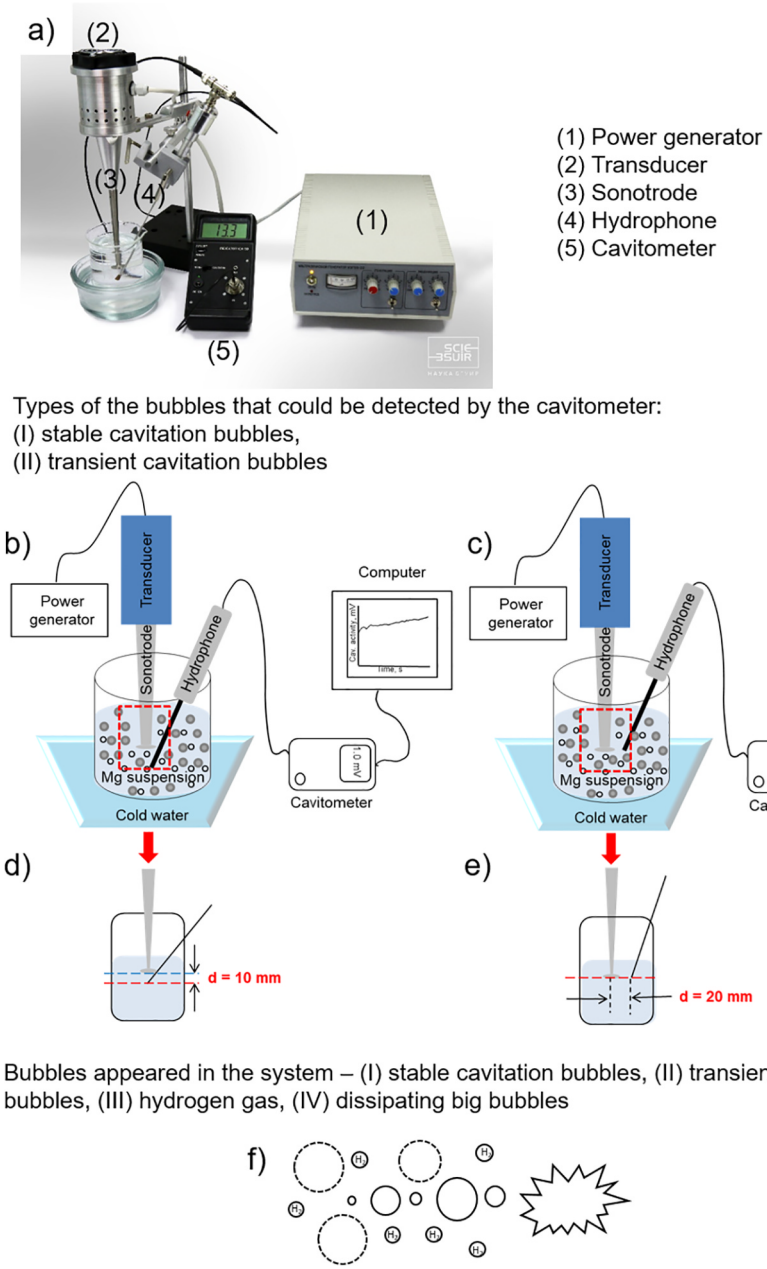

Fig. 1. Photo of the sonochemical setup (a). Schematic illustration of the setup indicating the different position of the hydrophone relative to the sonotrode: (b) under the sonotrode, (c) on the same level with the sonotrode tip. The illustrations (d, e) demonstrate the simplified schemes of the images (b, c) for Mg suspensions and liquids without particles and will be included next in the discussion. The question is: can generated hydrogen bubbles during ultrasonic treatment of magnesium particles participate in the evolution of stable or transient cavitation bubbles? (f).

($\lambda = 0.15418$ nm) at a scanning speed of 0.3°/min with a measurement range of 10–85°. For the determination of the instrumental broadening in the analysis of crystallite size, LaB_6 single crystal was used as a standard. The crystallite size was calculated using Scherrer Eq. (1):

$$D = K\lambda/\beta cos\theta \quad (1)$$

where D is the crystallite size (nm), K – shape factor, λ – wavelength of the radiation (nm), β – full width at half maximum of the peak with considering the instrumental broadening ($\beta = \beta_{sample} - \beta_{LaB6}$), θ – Bragg angle

2.2.3. Thermal analysis

Thermal analysis of the samples including thermal gravimetry (TG), differential thermogravimetry (DTG) and differential scanning calorimetry (DSC) was performed using a Netzsch STA 449 F3 thermal analyzer in a temperature range from 30 to 500 °C in air with heating speed of 10°min^{-1}

3. Results and discussion

Studying of the evolution of the cavitation bubble in magnesium suspensions is of interest, since this system provides the saturation of the electrolyte with hydrogen gas during the sonochemical treatment. It is a known reaction between the reactive metal (magnesium) and water [24]. This reaction is also used for hydrogen production from magnesium alloys [25]. Magnesium is an alkaline earth metal that is placed in the reactivity series after such metals as potassium, sodium and calcium (the most reactive metals that react with water very vigorously replacing hydrogen) as shown in Eq. (2).

$$Mg + 2H_2O = Mg(OH)_2 + H_2\uparrow \quad (2)$$

After immersing magnesium particles in water, the reaction of the production of magnesium hydroxide and release of hydrogen starts immediately. In turn, it is known [26–28] that the effectiveness of cavitation depends on the presence of dissolved gases and trace elements in the electrolyte, which determine the formation of cavitation bubble nuclei. However, we assume the cavitation activity depends on magnesium particles in a complex manner. At first, the more concentration of the magnesium particles is, the more hydrogen will be released. But this reaction leads to the formation of nanoscale brucite that serves as a matrix for chemically-binded released hydrogen reducing its amount in the electrolyte. In this regard, we varied the concentration of the magnesium particles in the electrolyte to study the evolution of the cavitation activity. Another parameter was the content of the organic solvents in the electrolyte because of its different ability to dissolve gases [29–31]. All measurements were performed 3 times for controlling the reproducibility of the measurements. The presented data are the average curves of 3 independent experiments. Example of typical reproducibility is shown in Fig. S1: spectra repeated each time.

3.1. Cavitation activity of aqueous suspensions with Mg particles

The records for different conditions are shown in Figs. 2, 3 and 7–12. From these figures it is seen, the activity of transient cavitation (A_{tr}) is not constant during processing and varies over a wide range.

Fig. 2 shows the results of experiments, which were performed with aqueous suspensions at different content of magnesium microparticles (C = 0.003 g/mL, 0.007 g/mL, 0.010 g/mL). As follows from the data presented, the A_{tr} value is maintained at a lower level for suspensions with higher particles concentrations during the entire period of recording.

Three stages of the evolution of the cavitation zone are distinguished here (Fig. 2a): 1 – the initial increase of cavitation activity, 2 – reaching a maximum with a subsequent decrease, and 3 – reaching the plateau (or the repeated cycles with feedback loops of enlargement/reduction of the cavitation activity).

The maximum cavitation intensity in the case of suspension with the particles content 0.003 g/mL comprised *ca.* 19 mV, for 0.007 g/mL – 11 mV and for 0.01 g/mL – 8.5 mV. Such a reduction in the values of the cavitation intensity can be related to the active production of cavitation bubbles and their transformation into the big ones (as a result of the rectified diffusion). In addition, with the increase of the Mg particle content in the suspension the maximum point appeared earlier.

To explain the low level of cavitation activity at the beginning of the experiment, we pay attention to the following. When magnesium particles were introduced into water, intense hydrogen evolution started releasing in the form of gas bubbles on the surface of particles. That is, the number of cavitation nuclei sharply increased in a liquid. Particles by itself may also serve as nuclei. Therefore, when ultrasound was turned on, the cavitation region may be in a state of oversaturation with bubbles. This state was previously discussed in [32–34].

The decrease in cavitation activity in the state of oversaturation is essential due to the screening action of the cavitation field and bubble–bubble impact. An increase in the intensity of bubble interactions and a simultaneous increase in bubble concentration can amplify the probability of bubble spherical form deformation at the early stage of collapse. As a result, interactions may be one of the factors which promote decreasing the cavitation activity in such conditions. Using a high-speed camera, we have observed a lot of small bubbles (Fig. S2). We suggest, the bubble formation could be explained by the decrease of the tensile stresses [35] and by the interaction with the propagating shock waves from the collapsing bubbles [36]. In addition, the tensile strength of the liquid is greatly weakened with increasing the volume concentration of big bubbles. As a result, no significant tensile stresses sufficient for the activation of bubbles with small sizes (of the order or less than the resonant size) can be achieved in it. We could observe the bubbles of different radii (from 5 μm to 160 μm, Supplementary Materials, Figs. S2, S3). In accordance with literature data [37], the resonant size of the bubble at the intensities of the order of cavitation

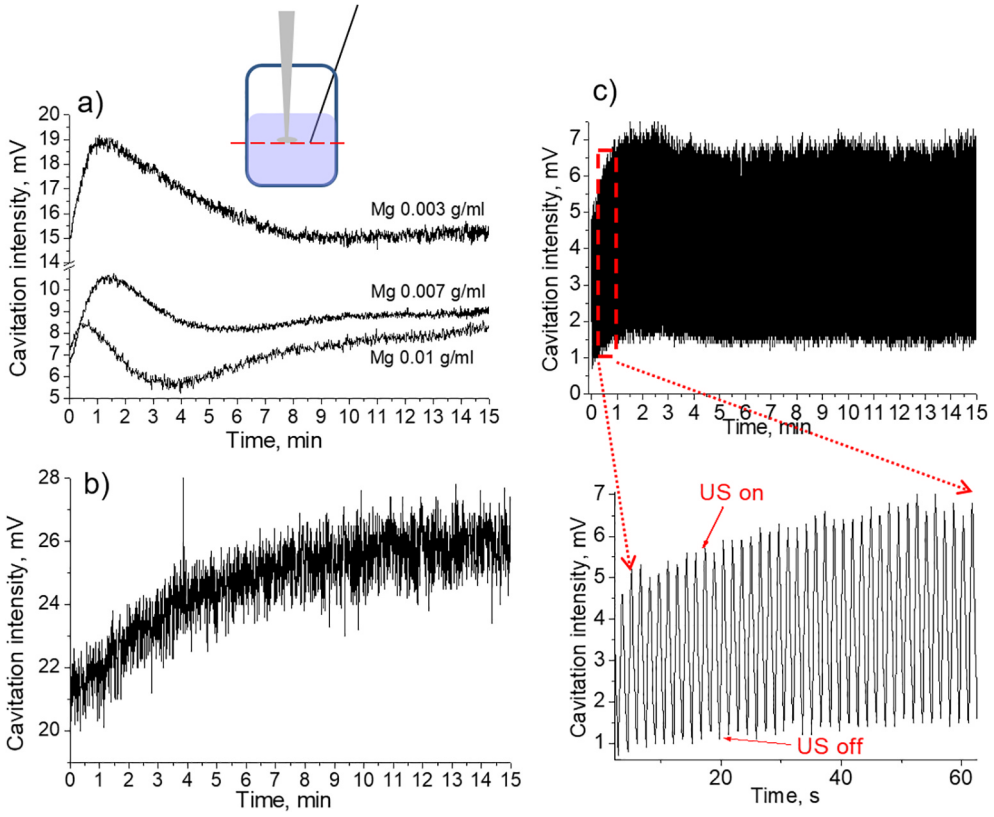

Fig. 2. Transient cavitation alteration for Mg aqueous suspensions with different particle content (a), distilled water (b). Curve presented on the plot (c) was measured in the pulsed regime of the sonication. The measurements were performed on the one level with the sonotrode tip (presented schematically on the top of the illustration).

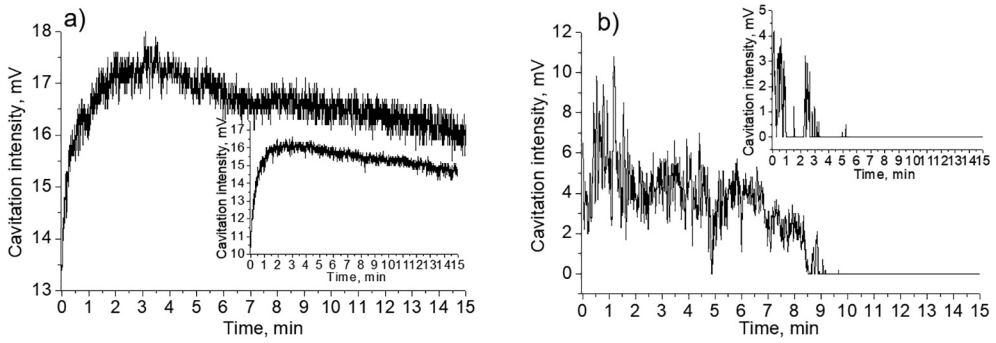

Fig. 3. Cavitation curves of Mg suspension in ethanol (a) and ethylene glycol (b), concentration 0.003 g/mL. The insets correspond to the cavitation activity measurements in pure liquids without particles.

threshold theoretical and experimental results showed that the ambient radius of the cavitation bubbles comprised 10–20 μm, the maximal size, to which it could extend before the collapse occurred, was estimated to be less than 90 μm. Thus, the bubbles of bigger sizes (Supplementary Materials, Fig. S2) with R > 40 μm could be attributed to the resonant bubbles. And finally, the third factor is the high gas content inside bubbles, which greatly dampens pulsations and collapse. Using a high-speed camera, we have observed bubble dynamics (Figs. S3 and S4, videos S1–S4). Gaseous hydrogen has the highest diffusivity in comparison with other gases [38] and actively participated in the process of gas saturation inside the bubble.

With increasing concentration of magnesium particles in suspension, the concentration of hydrogen bubbles increased as well. As a result, the cavitation activity is lower in suspensions with higher particle concentrations (Fig. 2a).

When ultrasound is turned on (first stage), stable bubbles could coalescence into big ones and they may float up or be removed from cavitation zone by acoustic streaming, *i.e.* the process of degassing was switched on. This is indirectly confirmed by the fact that when ultrasound was turned on, a large number of pop-up bubbles were observed on the surface of the suspension. As a result, the surface resembled the foam of an oxygen cocktail. This fact was a justification of oversaturation of cavitation zone. Unfortunately, the suspension was non-transparent and therefore the process of bubble formation and degassing could not be detected by optical methods.

Gradually, the cavitation zone became less saturated by bubbles. As a result, the conditions for initiating transient cavitation were improved. Therefore, cavitation activity increased at the first stage of sonication.

The decrease of the cavitation activity at the second stage was possibly associated with increased hydrogen release as a result of sound-chemical treatment of the particle surface. On the third stage the alterations of the cavitation activity in the case of 0.003 g/mL Mg aqueous suspensions were not significant as in suspensions with bigger concentration of particles. Reaching the plateau value may be explained by the stabilization of gas formation near the surface of magnesium particles. However, in these cases the stage of decrease of the cavitation intensity was followed by the repeat increase in cavitation intensity. In the case of ultrasonication of distilled water, (Fig. 2b) cavitation activity gradually increased in time.

For additional confirmation of a specific alteration of cavitation activity in Mg aqueous suspensions, the ultrasonic treatment of the

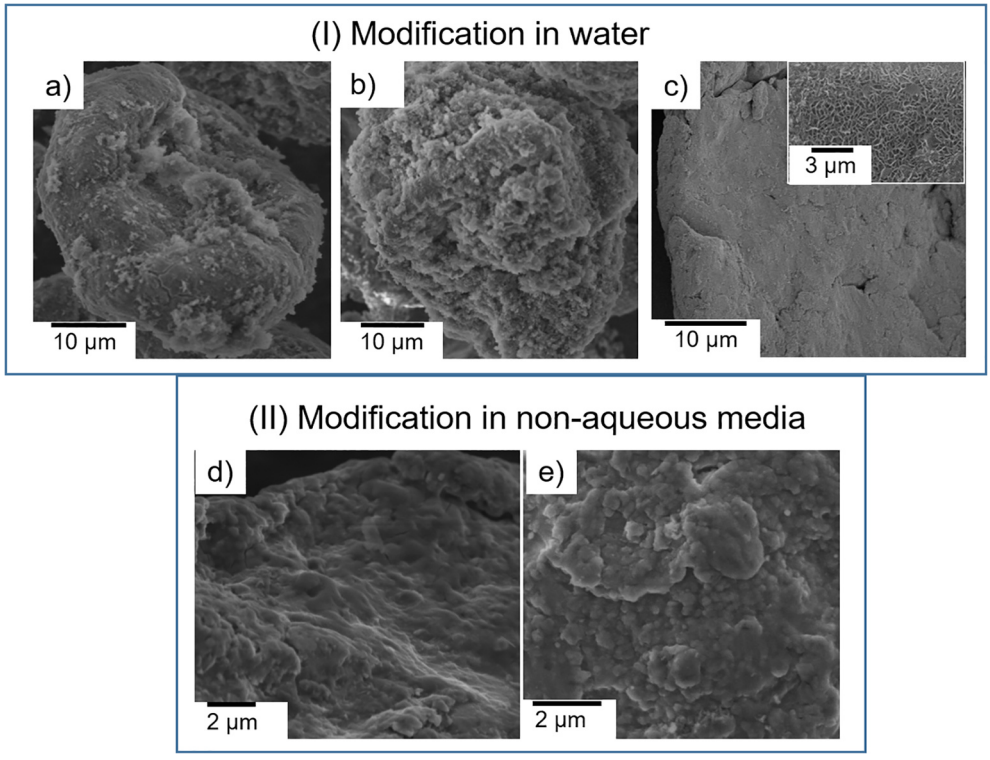

Fig. 4. SEM images of the Mg particles of 0.003 g/mL (a) and 0.010 g/mL (b) sonochemically treated aqueous suspensions. Microphotograph (c) denotes to the surface of the initial particle and inset corresponds to the particle treated in water in the absence of ultrasound (0.003 g/mL suspension). d) SEM images of Mg particles after sonochemical treatment of 0.003 g/mL suspensions in ethanol (d) and ethylene glycol (e). In all cases the duration of treatment comprised 15 min.

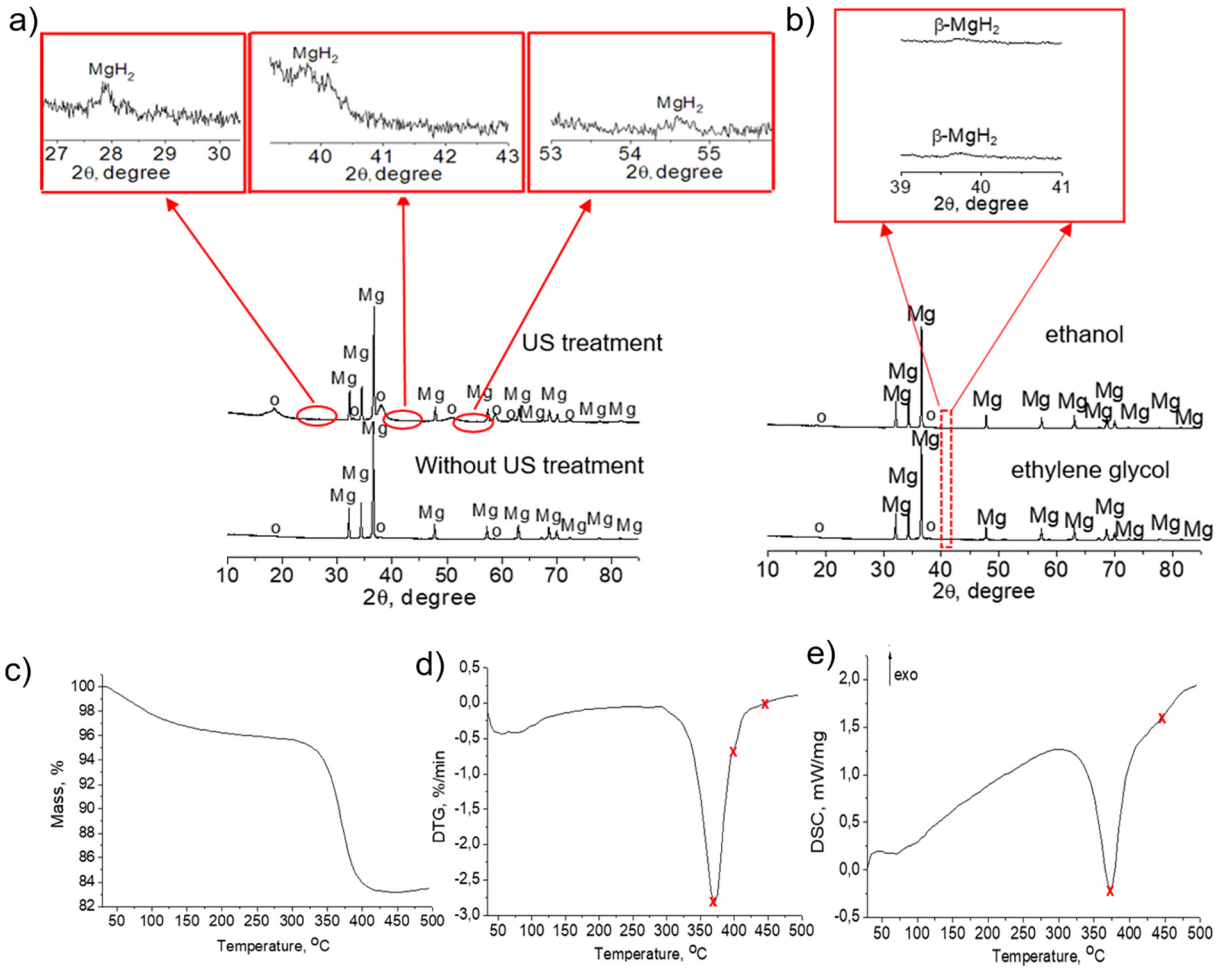

Fig. 5. XRD patterns of the Mg particles treated in water (a) in the presence/absence of ultrasonic impact, b) in ethanol or ethylene glycol, respectively. The symbol "o" corresponds to the brucite phase, the arrows are attributed to the magnification of the regions of the magnesium hydride reflexes which were detected in the samples after sonication. The duration of treatment comprised 15 min. Thermal analysis of the sample ultrasonically treated in Mg aqueous suspension during 15 min (c – TG curve, d – DTG curve, e – DSC curve, the arrow shows the direction of the exothermic processes). The symbol X corresponds to the designation of the main peaks of $Mg(OH)_2$ and MgH_2 decomposition.

suspension is performed using pulsed regime. This regime allows controlling the dynamics of cavitation activity [33,39]. First of all, we noted that in a pulsed field the level of cavitation activity achieved was significantly lower than in a continuous one. This may be due to the fact that the coalescence of bubbles slowed down, the rate of their association into large bubbles, that could float up or be carried to the surface of the liquid by acoustic currents from the cavitation zone, decreased. As a result, in a pulsed field the degassing rate decreased, the volume concentration of the bubbles remained higher for longer period. This, as noted above, had a negative effect on the transient cavitation activity.

Still the tendency of observing the maximum of cavitation intensity at the initial stages remained (Fig. 2c). Possibly, regardless the used mode of applied ultrasonic field the released hydrogen gas participated in the evolution of cavitation bubbles activity. The maximum activity of cavitation was not so pronounced as in the case of continuous field.

We carried out experiments with metal particles with lower chemical activity. Earlier, the influence of chemical activity of the ultrasonically treated material on its surface morphology was investigated [14]. In our study, we would like to discover whether it would be possible to observe the same effects in suspensions of less chemically active metals with the same concentration of metal particles. The higher level of cavitation activity was observed than in suspensions with magnesium particles in the moment of switching the ultrasound on. In the case of aluminium – the metal that follows magnesium in the reactivity series – the effect of the pronounced maximum at the first minutes of ultrasonic treatment (as observed in the case of magnesium) was not detected (results are shown in Supplementary materials) as in comparison with magnesium particles. During ultrasonic treatment of titanium as one of the most chemically resistant metals the cavitation activity was very close to the pure water (Fig. S5). During ultrasonic treatment of pure water without particles such maximum of the cavitation activity specific for Mg aqueous suspensions was not observed. Instead of this, a gradual growth of the cavitation activity with reaching a plateau value was detected. Thus, it can be concluded that chemical reactivity of the treated particles as the possibility to interact with water releasing hydrogen strongly influences the cavitation activity during sonochemical modification.

3.2. Cavitation activity in organic dispersion medium

In ethanol, in the moment of switching the ultrasound on, the small bubbles were observed due to the better solubility of gases in organic solvents in comparison with pure water [40]. The soluble gases facilitated the formation of cavitation nuclei and the density of bubbles in the cavitation zone. Because of the degassing during the ultrasonic treatment of the liquid, cavitation activity varied.

In the case of ultrasonic treatment of suspension of Mg particles (Fig. 3 a) in ethanol, we observed the cavitation activity variation similar to that in pure liquid (inset, Fig. 3a). However, a difference

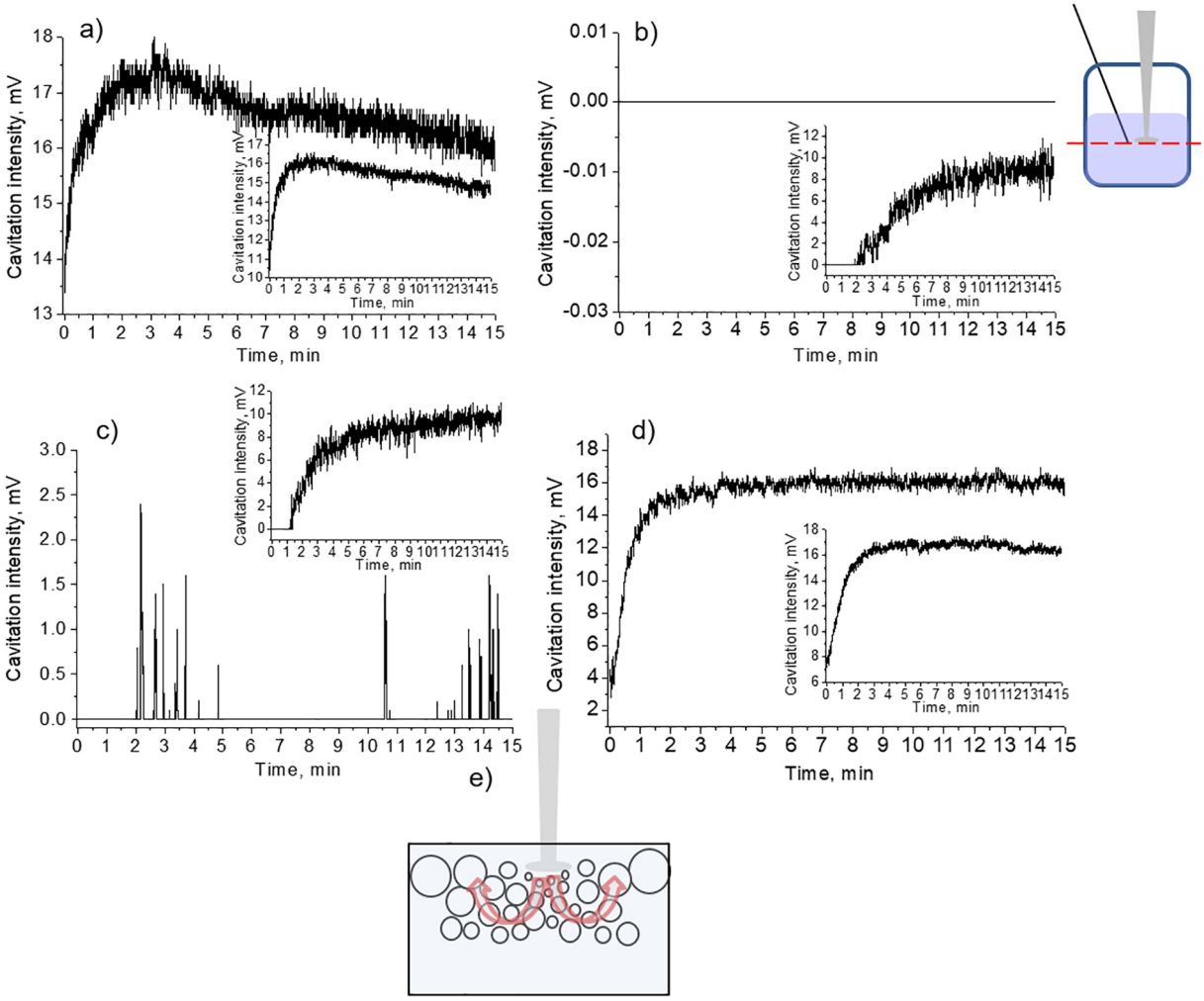

Fig. 6. Transient cavitation analysis for Mg suspensions in ethanol–water mixtures measured by hydrophone located on the same level with the sonotrode: a) pure ethanol, b) 20 vol% ethanol – 80 vol% water, c) 50 vol% ethanol – 50 vol% water, d) 80 vol. %ethanol – 20 vol% water. Scheme e) illustrates the movement of the big cavitation bubbles to the liquid/air interface. Insets correspond to the measurements in the liquids without particles. The concentration of Mg particles comprised 0.003 g/mL in all experiments.

between these two recordings can still be observed. During the first 6 min of ultrasonic treatment of the suspension, the maximum of the curve was more pronounced compared to pure liquid. In the case of treatment of glycolic suspension of the particles (Fig. 3b), the first 9 min of the sonication were characterized by gradual decrease of the cavitation activity whereas for pure liquid (inset, Fig. 3b) only the splashes of the recorded signal were initially observed. The photos demonstrating the shape oscillations of cavitation bubbles in different electrolytes are shown in Figs. S3 and S4. It should be mentioned that different solvents affect the size and the shape of the bubbles. For example, in water the radius of bubbles driven at a frequency of 20 kHz was ranging from 10 μm to 160 μm. Besides, there were different shape oscillations in water whereas in ethanol the shape of the bubbles did not differ significantly during the time (Supplementary materials, Fig. S2). The size of the bubbles in ethanol–water solutions was much smaller ($R_{max} < 100$ μm). This effect may be due to different solubility of gases in solvents [41] and different surface tension in different solvents [42]. The liquid inertia is also known to be a dominant factor affecting the bubble growth [43]. Besides, the nature of the electrolyte also affects the bubble size because the formulae describing bubble behavior include liquid density [44].

We relate the different behavior of cavitation activity in different liquids with the solubility of gases in different liquids. For instance, the solubility of oxygen at 25 °C in pure ethanol is *ca.* 10 times higher than in pure water [45]. Ethanol has lower surface tension, higher vapor pressure. Initial higher content of the dissolved gases may take part in the deceleration of the processes with Mg particles that occur in water. However, our experiment was limited to 15 min and we explained the reason for this limitation – avoiding overheating of the sonicated suspensions and obtaining reproducible curves of cavitation activity.

Ethylene glycol is a viscous liquid where the cavitation threshold is higher, cavitation activity without particles is low. Also, floating of the bubbles in ethylene glycol is inhibited and the bubbles remain under the sonotrode for a longer time.

The reason for the prolonged activity of the cavitation bubbles can also be explained by the influence of the released hydrogen resulting from the interaction between magnesium and trace amounts of water in the organic solvents. The system was saturated with hydrogen gas during the treatment.

3.3. Characterization of the sonochemically treated Mg particles

It is also worth mentioning the physicochemical transformations of the metal occurred during the ultrasonic treatment of magnesium microparticles. The chosen parameters of the ultrasonic treatment lead to the formation of magnesium hydride phase in aqueous medium. The less amount of sonication (less than 15 min) or the lower amplitude (less than 75%) did not result in the chemical binding of the released

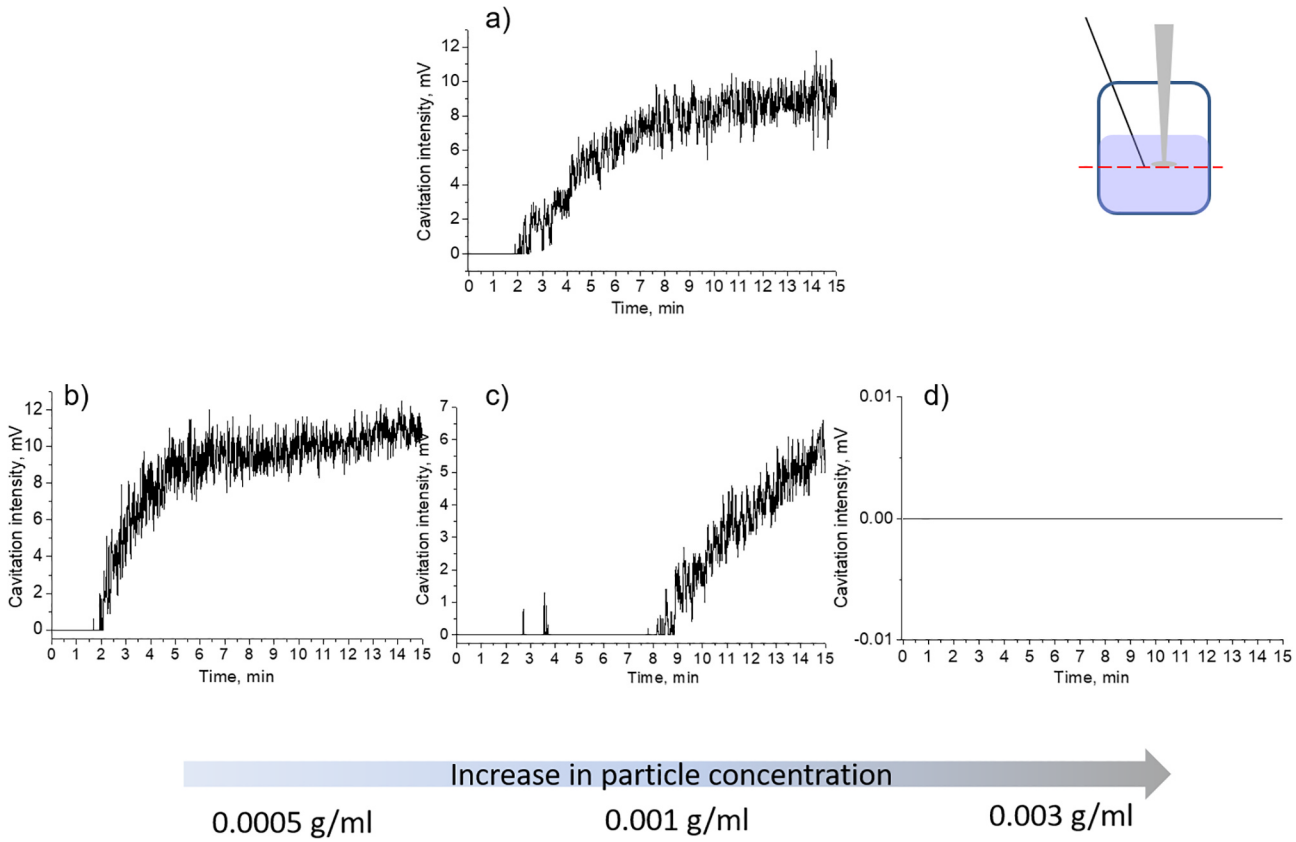

Fig. 7. Cavitation activity measurements for Mg suspensions in ethanol–water mixture (20 vol%-80 vol%) with different particle concentration. Curve a) corresponds to pure liquid, b) 0.0005 g/mL suspension, c) 0.001 g/mL suspension, d) 0.003 g/mL suspension.

hydrogen and the formation of magnesium hydride phase. The greater time of sonication did not provide good reproducible results for registration and analysis of the cavitation activity.

Analysis of the particle surface morphology before and after ultrasonic treatment showed that the surface is either partially (Fig. 4a) or completely (Fig. 4b) covered with a layer of magnesium hydroxide represented by dense or loose aggregates. Such difference in the surface morphology of the treated Mg particles can be explained with our cavitation measurements. In the cases of suspension with smaller concentration of particles (0.003 g/mL) the cavitation activity was higher, microjets and shock waves took part in an intensive process of the removal of the formed hydroxide aggregates.

We correlate the analysis of US-modified Mg particles morphology with the cavitation activity curves. In accordance with Fig. 2a, the cavitation activity for 0.003 g/mL suspension was higher than for suspensions with higher concentration of particles. This allows us considering that microjets and shock waves acted more intensively on the surface of the treated particles and the aggregates were removed. For the suspension with the particles concentration 0.010 g/mL the cavitation was lower and the morphology of the particles differed. The cavitation activity was lower and the action of microjets and shock waves was not significant.

At the same time in the cases of Mg particles obtained by the ultrasonic treatment of aqueous suspension with higher amount of the particles (0.010 g/mL) cavitation activity was smaller and the “abrasive” effect of microjets and shock waves was not so significant. The surface of the particles, free from such aggregates, was additionally covered with a layer of hydroxide due to the easy oxidation of reactive magnesium in air. In the case of magnesium particles treated in water in the absence of ultrasound (Fig. 4c, inset) the surface was evenly covered with a thin layer of native magnesium hydroxide, which was formed due to the “natural” oxidation of particles in water.

Describing the influence of non-aqueous media on the physicochemical properties of the modified Mg particles it was observed that US modification led to the formation of smooth surface layer (treated in ethanol, Fig. 4d) or aggregated (treated in ethylene glycol, Fig. 4e) layer.

The difference of the erosion patterns could be related with the difference of cavitation activity. It is interesting, that despite the speed of the sound is much higher in ethylene glycol (approx. 1616 $m \cdot s^{-1}$ [46]) compared to water (approx. 1500 $m \cdot s^{-1}$ [46]) and ethanol (approx. 1180 $m \cdot s^{-1}$ [47,48]) the cavitation activity in the ethanol suspension of Mg particles was higher than in the case of ethylene glycol suspension (Fig. 3). That’s why we can assume that the impact of shock waves and microjets in ethanol suspension was higher and the surface of the ultrasonically treated particles was presented with a smooth layer. In the case of glycol suspensions, the erosion pattern of the particle was presented with the aggregates, the cavitation activity was lower than in the case of ethanol and the driving force to remove the aggregates was not so active.

It should be mentioned that even in the cases of using organic dispersed media, in our experiments (ethanol and ethylene glycol), little water content (several percent) presented in the sonicated system and interacted with magnesium particles. However, it is known that ethanol and ethylene glycol can act as scavengers of the hydroxyl radicals [49] formed during ultrasonic treatment in aqueous conditions. Thus, the use of organic medium prevented the oxidation of the magnesium surface and the formation of platelet-like structure of $Mg(OH)_2$ that was formed during US treatment in water. The presence of the magnesium hydroxide and hydride was confirmed by XRD analysis (Fig. 5). In the case of the samples treated in water without ultrasound (chemical oxidation) magnesium hydroxide was formed in trace amounts. MgH_2 phase was not detected compared to US-treated samples. According to the diffraction patterns of the samples treated in water, the reflexes in

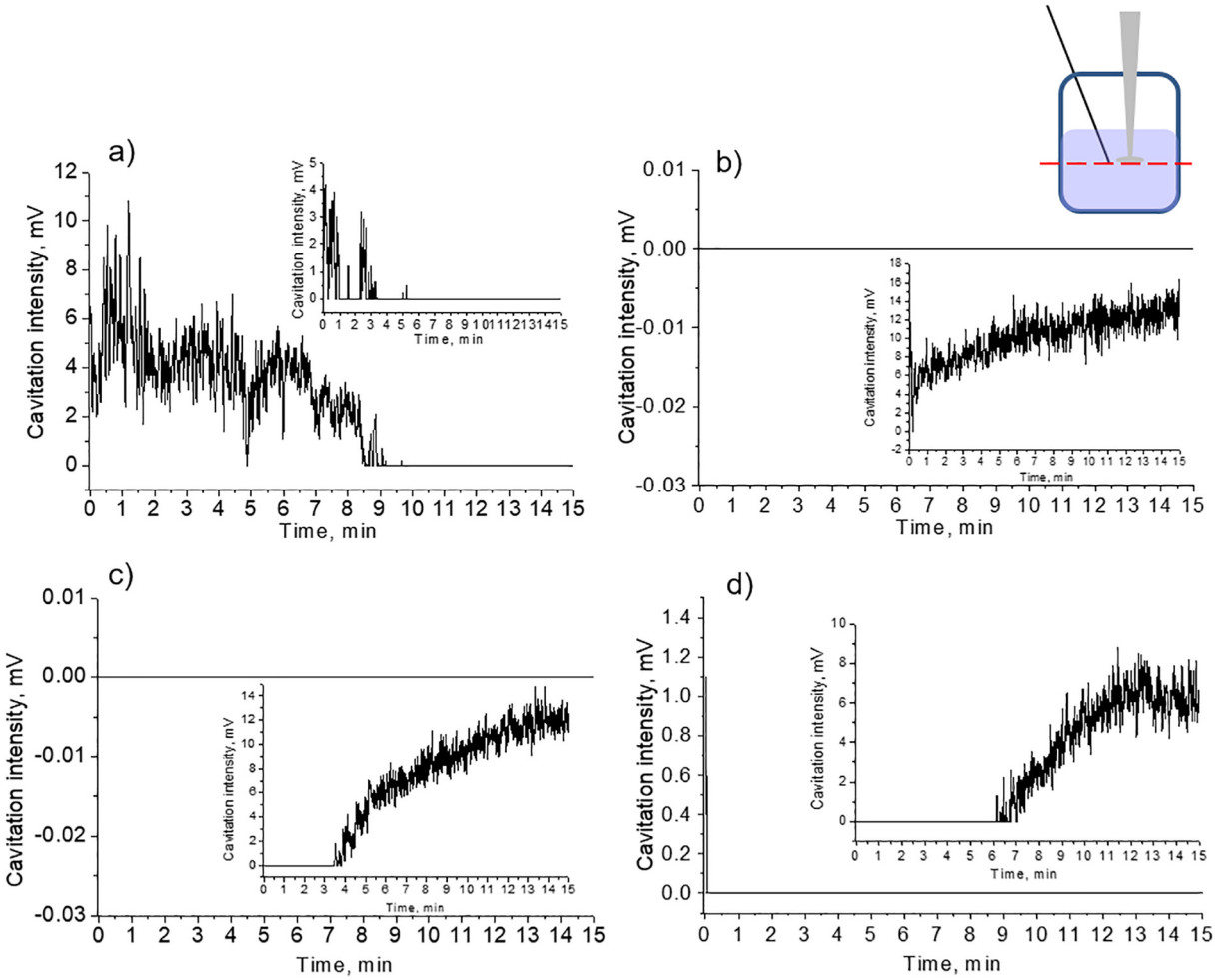

Fig. 8. Transient cavitation analysis for Mg suspensions in ethylene glycol–water mixtures measured by hydrophone located on the same level with the sonotrode: a) pure ethanol, b) 20 vol% ethylene glycol – 80 vol% water, c) 50 vol% ethylene glycol – 50 vol% water, d) 80 vol% ethylene glycol – 20 vol% water. Insets correspond to the measurements in the liquids without particles. The concentration of Mg particles comprised 0.003 g/mL in all experiments.

the region of 2θ: 18.2°, 32.8°, 37.7°, 50.8°, 58.7°, 62.1°, 72.3° corresponded to the brucite phase (ICDD № 44-1482), and peaks at 27.8°, 35.8°, 54.5° were attributed to the hydride (ICDD № 12-0697). The peaks of 39.8°, 49.4°, 50.9°, 72.2° were attributed to the high-temperature β-MgH_2 phase (ICDD № 35–1185), however the peaks at 49.4°, 50.9°, 72.2° were not clearly distinguished among the main reflexes of magnesium and magnesium hydroxide. This fact can confirm the possibility of ultrasonic treatment method to form high-temperature phases resulting from the high temperatures and pressures zones near the bubble collapse. It is assumed that hydride structure can be stabilized inside the magnesium-brucite basis and remain its stability regardless the chemical property of MgH_2 to be rapidly decomposed in the presence of water.

The average crystallite size of $Mg(OH)_2$ calculated by Scherrer equation was estimated to be 9, 15 and 12 nm for Mg suspensions 0.003 g/mL, 0.007 g/mL and 0.010 g/mL, respectively (Table S1). These calculations confirm the formation of nanoscale magnesium hydroxide prepared by ultrasound-assisted method. For particles treated in ethanol and ethylene glycol (Fig. 5b), XRD analysis confirmed that $Mg(OH)_2$ phase was presented only in trace amounts. In addition, the presence of high-temperature β-MgH_2 phase was also observed.

The presence of MgH_2 and $Mg(OH)_2$ in the sonicated samples was

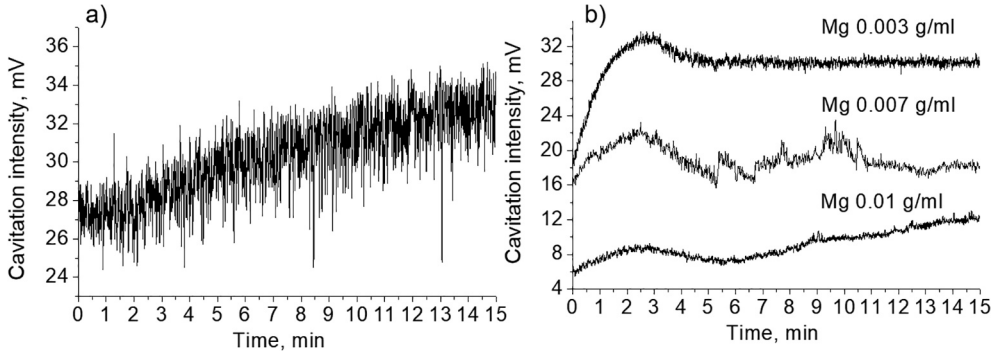

Fig. 9. Transient cavitation curves measured for water (a) and Mg aqueous suspensions (b) by hydrophone located under the sonotrode.

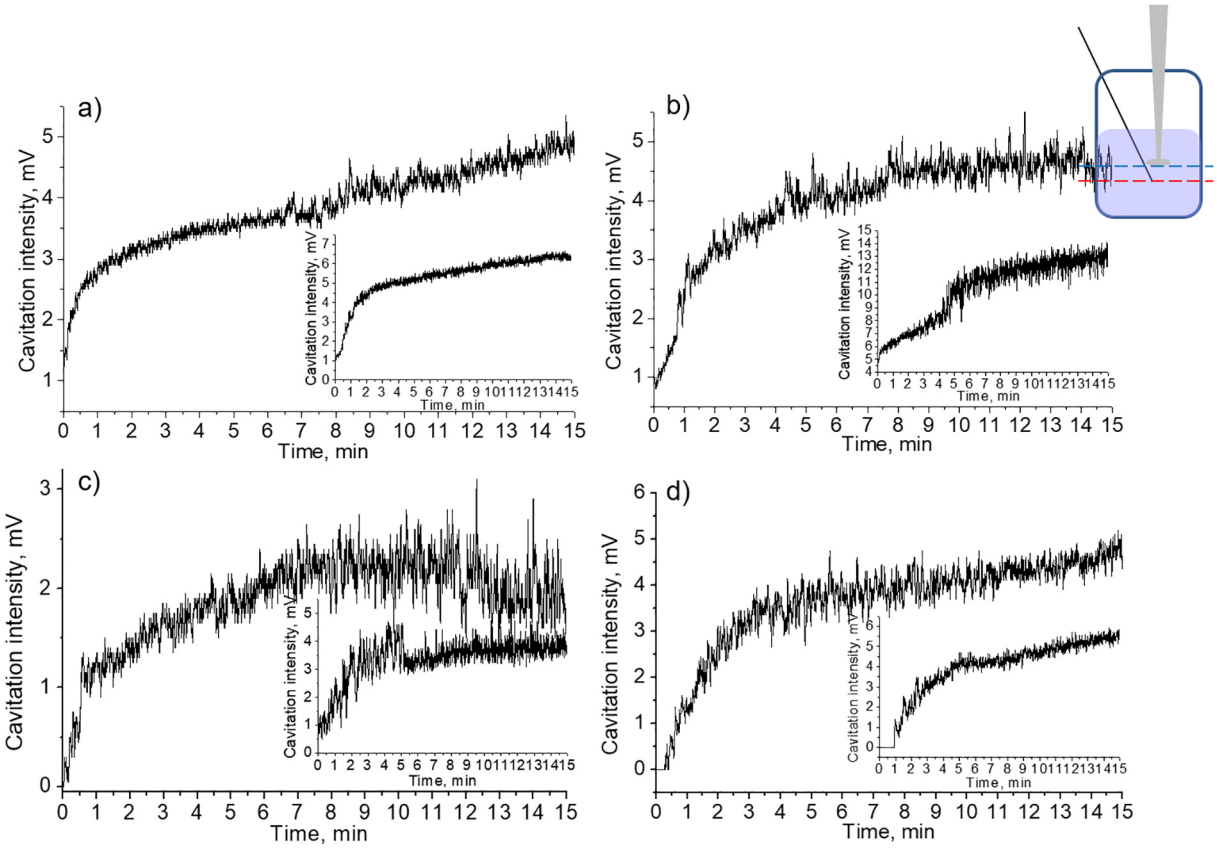

Fig. 10. Transient cavitation analysis for Mg suspensions in ethanol–water mixtures measured by hydrophone located under the sonotrode: a) pure ethanol, b) 20 vol % ethanol – 80 vol% water, c) 50 vol% ethanol – 50 vol% water, d) 80 vol% ethanol – 20 vol% water. Insets correspond to the measurements in the liquids without particles. The concentration of Mg particles comprised 0.003 g/mL in all experiments.

also detected by thermal analysis (Fig. 5 c). By means of thermogravimetry (TG) it was estimated that during heating up to 500 °C the mass loss comprised ~12% (Fig. 5d). Heating the sample up to 100–150 °C was accompanied by the desorption of the physically adsorbed water. Differential thermogravimetry (DTG) indicated two separated peaks in the regions 371 °C and 399 °C (Fig. 5d) which could be attributed to the decomposition of $Mg(OH)_2$ and MgH_2, respectively (the Eqs. (3) and (4) are given below).

$$Mg(OH)_2 \rightarrow MgO + H_2O \quad (3)$$

$$MgH_2 \rightarrow Mg + H_2 \quad (4)$$

Differential scanning calorimetry (DSC) indicated an endothermal peak starting at 344 °C and finished at 400 °C (Fig. 5e) that can be attributed for the simultaneous decomposition of the hydroxide and hydride phases in this temperature region. Also, the second broad small endothermal peak centered at 440 °C can be the confirmation of the second stage of hydrogen desorption from the magnesium hydride that is formed during ultrasonic treatment in aqueous conditions [10].

3.4. Cavitation activity in organic-aqueous suspensions of Mg particles and different hydrophone positions

To investigate the cavitation activity of magnesium suspensions more thoroughly, we carried out experiments with different positions of the hydrophone and in organic-aqueous suspensions with different water content.

The most important stages in the cycle of the transient cavitation bubble include 1) nucleation followed by the rapid growth of the bubble and 2) the collapse followed by significant concentration of energy. For each of these steps the radius of the bubble must exceed some critical value [50]. The dynamics of the bubble is affected by the action of acoustic pressure, hydrostatic pressure, pressure of the gas–vapor mixture inside the cavitation bubble, surface tension that cause the complicated dependence of bubble radius with time [51]. The dynamics of the cavitation bubble is described with the following Eq. (5):

$$R\frac{d^2R}{dt^2} + \frac{3}{2}\left(\frac{dR}{dt}\right)^2 + \frac{1}{\rho}\left[P_\infty - P_{vap} - P_g + \frac{2\sigma}{R} + \frac{4\eta}{R}\frac{dR}{dt} - \left(P_\infty + \frac{2\sigma}{R_0}\right)\left(\frac{R_0}{R}\right)^{3\gamma}\right] = 0 \quad (5)$$

where R is the current radius of the bubble, P_∞ – hydrostatic pressure of the liquid, P_{vap} – vapor pressure, P_g – pressure of the gas inside the cavitation bubble, ρ – density of the liquid, σ – surface tension, η – viscosity of the liquid, R_0 – initial radius of the bubble [32].

The main parameters of the liquids used in our experiments – water, ethanol and ethylene glycol – are given in Table S2. In the case of using liquid ethanol–water mixtures, the bubble nuclei can appear due to the dissolved gases or microcontaminants, whereas in the case of Mg suspensions, the magnesium particles and released hydrogen served as a platform for cavitation bubble nucleation. The solubility of gases in water and ethanol or ethylene glycol is an important parameter that influences the formation of bubbles. Dissolved gases (taking into account mainly carbon dioxide, oxygen and nitrogen) influenced the rate of bubble nucleation, the nucleation rate increased with the amount of the gas [26]. The possible explanation of this phenomenon is the reduction of the surface tension. A lowered surface tension participated in the decrease of the tensile strength for bubble growth [52].

When adding water to ethanol, in the final solution the solubility of gases was lower than in the case of pure ethanol [40]. The solubility of gases in the prepared solution decreased and gas released in the form of

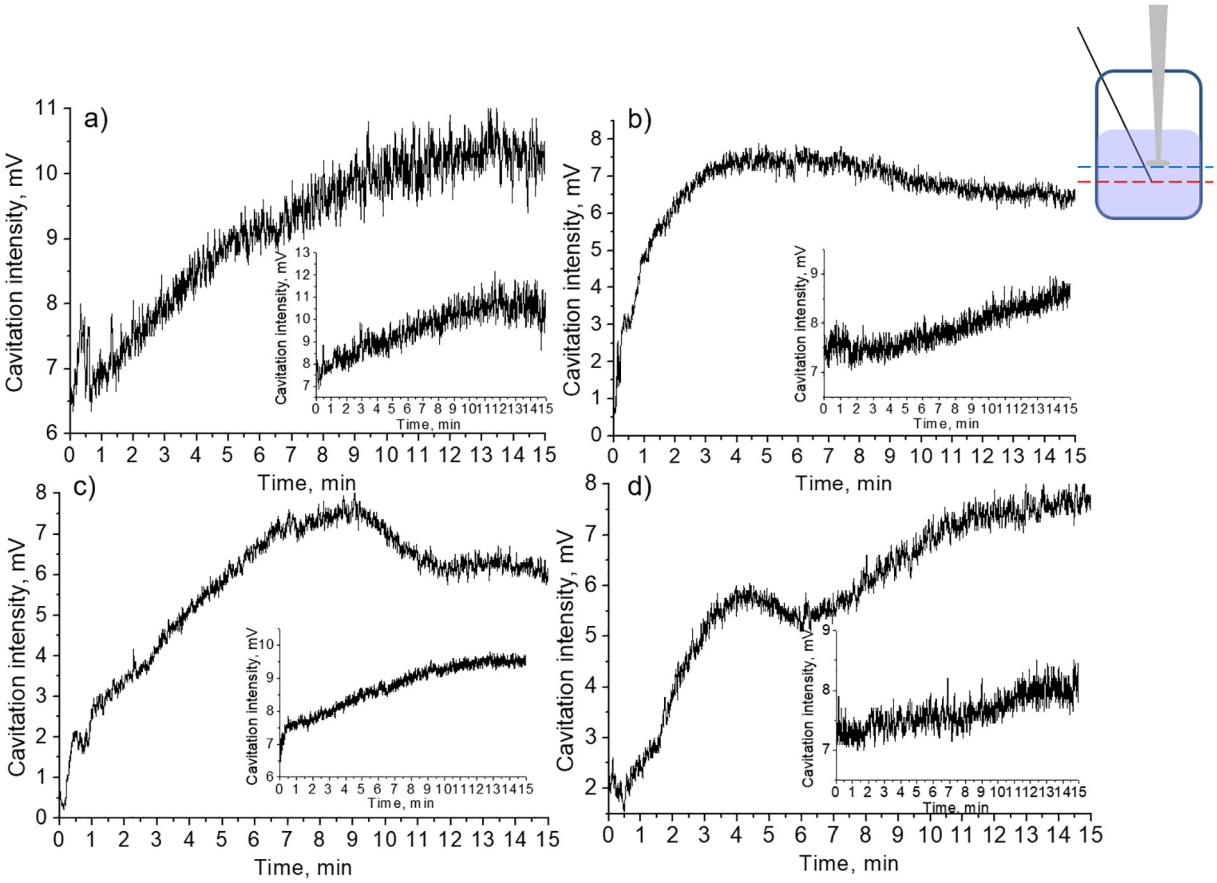

Fig. 11. Transient cavitation analysis for Mg suspensions in ethylene glycol–water mixtures measured by hydrophone located under the sonotrode: a) pure ethanol, b) 20 vol% ethylene glycol – 80 vol% water, c) 50 vol% ethylene glycol – 50 vol% water, d) 80 vol% ethylene glycol – 20 vol% water. Insets correspond to the measurements in the liquids without particles. The concentration of Mg particles comprised 0.003 g/mL in all experiments.

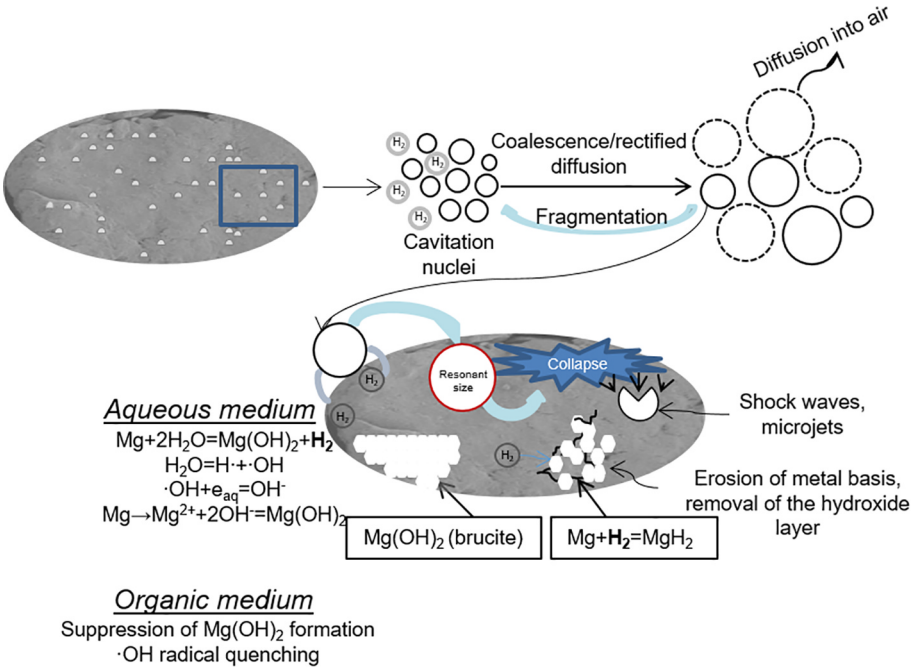

Fig. 12. Schematic illustration of the cavitation bubble evolution in the presence of Mg particles and the physicochemical transformations of the material and dispersed medium that takes place during ultrasonic treatment.

bubbles. Ultrasonic treatment facilitated this process, bubbles released rapidly and changed the transparency of the liquid.

In ethanol at the initial stage of ultrasonic treatment, the liquid became muddy due to the release of a great number of bubbles with the sizes less than 100 μm (R < 100 μm). As alcohol molecules prevent the mechanism of bubble growth by coalescence [53], the most probable formation of the big size-bubble or bubble clusters was rectified diffusion. Such structures prevented the formation of actively cavitating small bubbles and supersaturation of the cavitation zone with the described bubbles took place.

Interestingly, in the cases of ethanol–water mixtures with different ethanol content different cavitation activity was observed (Fig. 6). In the cases of predominant content of ethanol (pure ethanol and 80 vol%) cavitation activity was observed from the very beginning of ultrasonic treatment. In addition, the cavitation curves of the suspensions (Fig. 6 a, d) and the solutions (insets Fig. 6 a, d) were practically identical. However, in the cases of smaller content of ethanol (20 vol% and 50 vol %) a significant difference between the suspensions (Fig. 6 b, c) and ethanol-aqueous solutions (insets Fig. 6 b, c) was observed. For liquids without particles, the cavitation activity started to be detected after 1–2 min after switching the ultrasound on. For the suspensions with the abovementioned water-alcohol ratios the cavitation activity was either detected in the form of splashes during the period of sonochemical treatment (Fig. 6 c) or not detected at all (Fig. 6 b).

The physicochemical aspects of ethanol–water solutions with different water content should be mentioned. In the case of two initial liquids (separately, water and separately, ethanol) the hydrogen bonds between the molecules of one type (H_2O…H_2O or C_2H_5OH…C_2H_5OH) take place. When mixing ethanol and water with each other, the hydrogen bonds are destructed and the distances between initially bonded molecules H_2O…H_2O in water and C_2H_5OH…C_2H_5OH in ethanol, respectively, increase. This results in the enlargement of vapor pressure of the finite alcohol-water solution in comparison with pure solvents [54]. The formation of new hydrogen bonds between ethanol and water takes place. Thus, the mixtures of ethanol–water solutions are characterized by association/dissociation of hydrogen bonds between alcohol and water molecules influencing the main physicochemical parameters of the final solution. In addition, the structure of the “polymers” formed in ethanol-aqueous solutions can differ depending on the content of ethanol [55].

According to the literature data [56], starting from 8 mol.% of ethanol in aqueous solution (which is close to the value of 7.2 mol.% recalculated for 20 vol% (C_2H_5OH) − 80 vol% (H_2O) solution) strong self-association of H_2O molecules was reduced and predominant formation of ethanol–water molecular bonds occurred. At higher concentrations of ethanol (> 20 mol.% that correspond to the cases of 50 vol% (C_2H_5OH)-50 vol% (H_2O) and 80 vol% (C_2H_5OH)-20 vol% (H_2O)) the H_2O…H_2O bonds were broken and the formation of clustered structure with a stacked ethanol core and a thin shell of water occurred. Grieser *et al.* [53] revealed that for some sonochemical processes the amount of alcohol molecules adsorbed at the bubble-water interface influenced more significantly than the concentration of alcohol in bulk solution. Another study of the multibubble sonoluminescence in ethanol–water solutions [56] demonstrated that alcohols could act as luminescence quenchers and be responsible for the formation of bubble clusters.

Thus, we can conclude that the effect of the constant signal quenching was clearly observed in the case of 20 vol% (C_2H_5OH) − 80 vol% (H_2O) Mg suspension and thus cannot be related with the increase of the ethanol concentration in bulk solution. In the cases of Mg suspensions with lower content of particles, the cavitation activity in the suspension gradually became similar to pure solvents. Thus, in the Mg suspensions under consideration (Fig. 6 b, c), the hydrogen gas could influence the process of bubble growth to some extent, taking into account the presence of alcohol which molecules limit the growth of the bubbles by coalescence mechanism [53]. In this case, the structures of the bubbles can be presented either in the form of bubble clusters or in the form of the bubbles of big sizes grown by the mechanism of rectified diffusion. These structures floated to the liquid/air interface outside from the center of the sonotrode and screened the signal detection (the schematic representation is given in Fig. 6 e). Presumably, in the case of suspensions with higher content of ethanol (Fig. 6a, d) the influence of the released hydrogen (in less amount) was not sufficient as in the case of the suspensions with greater amount of water (Fig. 6b, c).

At the initial stages, the bubbles were formed very intensively, forming the big bubbles that moved from the central part under the sonotrode to the periphery. Gradually, the cavitation appeared and afterwards reached its equilibrium value with negligible fluctuations of the cavitation intensity. During the ultrasonic treatment of Mg particles in ethanol–water mixtures the formation of $Mg(OH)_2$ took place as the process of metal oxidation in the presence of water.

Previously, Tzanakis *et al.* [57] reported about the development of cavitation zone in various liquids. Particularly, the authors found out that in the case of water the conical cavitation bubble structures were formed whereas in ethanol they detected that bubbles have a tendency to be dispersed outside the cavitation zone and reach the free surface. In our cases we could detect the cavitation activity in the position under sonotrode both for liquids and for suspensions. Our results correlate with data [57], in case of water we detected the higher cavitation activity for the position under sonotrode and in ethanol the signal of cavitation detection was higher on the one level with sonotrode. The difference in cavitation activity between the liquids and the suspension can be explained by the influence of the released hydrogen bubbles described earlier. Big bubbles or clusters of the bubbles move from the zone directly under the sonotrode to the periphery zones (Fig. 6, e).

As described above transient cavitation activity for Mg suspension of the appropriate composition (20 vol% ethanol − 80 vol% water) we could not detect any signal of the hydrophone and this effect was reproducible. To check the influence of magnesium particles we studied the cavitation activity in ethanol–water mixture with different Mg particles content. Fig. 7, a showed that in the control experiment in pure liquid we detected the signal of the hydrophone starting from the 2nd min of the ultrasonic treatment. Gradually increasing the particle concentration in the treated suspension from 0.0005 g/mL to 0.0030 g/mL (Fig. 7, b-d) the delay of the cavitation activity detection was observed. The value of 0.0030 g/mL was a critical concentration when we could not detect the cavitation.

In the case of ethylene glycol–water mixtures with Mg particles we could observe cavitation intensity only in the case of pure ethylene glycol (Fig. 8 a). In other cases, (Fig. 8 b-d) the cavitation activity was not detected during the whole period of the treatment of the suspension. We assume that for the used concentration of the Mg particles in the suspension was critical to detect any transient cavitation activity in ethylene glycol–water solutions. In the current position of the hydrophone there was no zone of active bubbles that could be detected by the sensor. Here, the released hydrogen played a role in the processes of bubble clusters or big bubbles formation near the zone of the hydrophone (in comparison with liquids without particles we could observe the signal from the active cavitation bubbles (insets Fig. 8 b-d). Additionally, the abovementioned oversaturation of the zone near detector should be taken into account that the big bubbles formed from the penetration of hydrogen gas inside the cavitating bubble can interrupt the detection of the signal from the cavitating and collapsed bubbles. Additional experiments confirmed that concentration of Mg particles is essential for analysis of cavitation activity.

3.5. Position of the hydrophone under the sonotrode tip

Fig. 9 shows the obtained curves of changes in cavitation activity of the Mg aqueous suspensions with the concentrations described in the Section 3.1. The processes of the increase and decrease of the cavitation activity in the cases of suspensions with more Mg particles content

0.007 g/mL and 0.010 g/mL) were more pronounced in the current position of the hydrophone. The processes can be described in the same manner as in the case of another hydrophone position discussed above.

In the position of the hydrophone under the sonotrode tip in the ethanol–water mixtures (Fig. 10) we investigated the difference in the cavitation activity of pure liquids and with Mg particles. In the case of suspensions with larger ethanol (pure ethanol and 80 vol%) content the cavitation activity was very similar to that without the particles (Fig. 10 a, d). In the cases of the suspensions with a large water content (80 vol % and 50 vol%) (Fig. 10 b, c) we could observe the broad maximums on the cavitation curves whereas in the cases of liquids (insets Fig. 10) we could observe the gradual reaching of the equilibrium state with time.

Thus, we can conclude that Mg particles strongly influenced the development of the cavitation zone for ethanol and ethylene glycol aqueous mixtures.

In the case of pure ethylene glycol (Fig. 11 a) the cavitation alteration was very similar to that without particles (inset Fig. 11 a). In the cases of ethylene glycol–water mixtures (Fig. 11 b-d) we also detected the maximum in the cavitation activity, analogous to those observed in water. Moreover, with increasing the content of water in the suspension the following tendency could be observed – the maximums of the cavitation activity had the tendency to combine and form the broad maximum of the cavitation intensity. With the increase of the concentration of the released hydrogen the processes of active bubbles formation and their growth into the bubbles of bigger size were likely to occur in the continuous manner.

In addition, for the glycol–water based systems we could observe the cavitation activity 1.5–2 times higher than for ethanol–water solutions. For the explanation of this phenomenon another important parameter discussed in [58,59] should be taken into account. Alcohols and diols have different structure – namely, ethylene glycol has an extra –OH group in its composition and additional ability to form hydrogen bonds. Breaking the hydrogen bonds can be regarded as a rate-limiting step in the process of vaporization of such liquids [60]. If liquid forms more hydrogen bonds in its structure, then more energy will be needed for evaporation and consequent transfer inside the bubble. From this point of view, it is easier for ethanol to be evaporated from its solution and participate in the bubble growth, participating in the mechanism of the signal quenching.

3.6. Mechanism of cavitation bubbles evolution

The mechanism of the cavitation bubbles evolution and the modification of the metal particles can be presented as follows (Fig. 12). Initially, when adding the particles to the aqueous medium, the reaction between magnesium and water occurs. The metal surface is being oxidized and, finally, magnesium hydroxide is formed. Another product of the reaction includes hydrogen. These particles serve as a platform for the heterogeneous bubble nucleation. Afterwards, the cavitation nuclei grow in the presence of the released hydrogen bubbles and lead to the formation of small cavitation bubbles. The subsequent growth of the produced small bubbles by several mechanisms leads to the formation of big bubbles (described above). When reaching critical size, the bubbles collapse, producing shock waves, microjets and reactive oxygen species (ROS) that modify the surface of the treated material. In the cases of non-aqueous media [61–65], the decomposition of ethanol and ethylene glycol include the formation of H·, C_2H_5O· and $C_2H_5O_2$· radicals being the quenchers of the OH radicals.

To sum up, in the case of ultrasonic Mg treatment, the physicochemical processes include sonolysis of the dispersed medium, accelerated or inhibited oxidation of the metal basis with the simultaneous formation of magnesium hydride.

4. Conclusions

Evolution of cavitation activity bubbles during ultrasonic treatment of magnesium suspensions has been investigated. When studying the alteration of the transient cavitation during the modification of the material, it was investigated that the cavitation intensity can influence the properties of the modified magnesium particles (surface morphology, phase composition) and the products of sonochemical treatment of magnesium (particularly, released hydrogen gas) can influence the cavitation bubbles development. Generally, it is possible to distinguish the following stages of cavitation activity alteration: initially, the cavitation zone was oversaturated by gas bubbles with the sizes much larger than the resonant at an applied frequency, and the high volume concentrations of such big bubbles represents the difficulty to cavitating bubble formation. In the moment of switching the ultrasound on, the degassing of the liquid led to the removal of such bubbles and facilitate the process of real cavitating bubbles formation. The stage of decrease in cavitation activity can be associated with acceleration of hydrogen production and creating the conditions for active bubble–bubble interactions, and bubble collapse. The stage of reaching the plateau value can be related with the stabilization of the processes of bubbles formation/destruction.

Besides the fundamental understanding of cavitation processes, this work raises a question of the reactive gas bubbles formation for triggering novel nanostructured functional materials, here, for hydrogen storage. The sonochemical treatment in aqueous medium led to the formation of magnesium hydroxide and magnesium hydride. Particularly, the formation of brucite ($Mg(OH)_2$) resulted from the intensive oxidation of the metal substrate, whereas magnesium hydride was a confirmation of the possibility to bind hydrogen in the conditions of bubble collapse. In organic media (ethanol, ethylene glycol) the suppression of the brucite formation has been observed. Analysis of cavitation activity in organic-water mixtures confirmed that hydrogen gas *in situ* evolved from the ultrasonic modification of the material strongly influenced the cavitation bubbles behavior.

5. Author statement

NB performed all experiments, NVD helped with measurements of transient cavitation activity, SAU helped with magnesium ultrasonic treatment and did study of cavitation bubbles, EVS and NVD generated the ideas. All authors wrote the manuscript.

Declaration of Competing Interest

The authors declare that they have no known competing financial interests or personal relationships that could have appeared to influence the work reported in this paper.

Acknowledgments

The authors thank L. S. Ivashkevich (Research Institute of Physicochemical Problems, Minsk, Belarus) for the help with performing XRD analysis and L. I. Pan'ko, D. I. Shiman (Research Institute of Physicochemical Problems, Minsk, Belarus) for the help with performing thermal analysis of the samples. This work was financially supported by Russian Science Foundation, Grant No. 19-79-10244. ITMO Fellowship and Professorship Program 08-08 is acknowledged for infrastructural support.

Appendix A. Supplementary data

Supplementary data to this article can be found online at https://doi.org/10.1016/j.ultsonch.2020.105315.

References

[1] G. Chatel, J.C. Colmenares, Sonochemistry: from basic principles to innovative applications, Top. Curr. Chem. 375 (2017) 8, https://doi.org/10.1007/s41061-016-

0096-1.
[2] A. Baranchikov, V. Ivanov, Y. Tretyakov, Sonochemical synthesis of inorganic materials, Russ. Chem. Rev. 76 (2007) 133, https://doi.org/10.1070/RC2007v076n02ABEH003644.
[3] K.S. Suslick, G.J. Price, Applications of ultrasound to materials chemistry, Annu. Rev. Mater. Sci. 29 (1999) 295–326, https://doi.org/10.1146/annurev.matsci.29.1.295.
[4] B. Hidding, Sonochemistry of silicon hydrides, Science 360 (80) (2018) 489–490, https://doi.org/10.1126/science.aap8005.
[5] D. Lohse, Sonoluminescence: Cavitation hots up, Nature 434 (2005) 33–34, https://doi.org/10.1038/434033a.
[6] M.A. Margulis, Basics of sonochemistry. Chemical reactions in the acoustic fields (in Russian), "High school," Moscow, 198.
[7] I. Tzanakis, M. Hodnett, G.S.B. Lebon, N. Dezhkunov, D.G. Eskin, Calibration and performance assessment of an innovative high-temperature cavitometer, Sensors Actuat. A Phys. 240 (2016) 57–69, https://doi.org/10.1016/j.sna.2016.01.024.
[8] B.K. Kang, M.S. Kim, J.G. Park, Effect of dissolved gases in water on acoustic cavitation and bubble growth rate in 0.83 MHz megasonic of interest to wafer cleaning, Ultrason. Sonochem. 21 (2014) 1496–1503, https://doi.org/10.1016/j.ultsonch.2014.01.012.
[9] P.W. Mertens, M. Hauptmann, H. Struyf, P. Mertens, M. Heyns, S. De Gendt, C. Glorieux, S. Brems, Towards an understanding and control of cavitation activity in 1 MHz ultrasound fields, Ultrason. Sonochem. 20 (2013) 77–88, https://doi.org/10.1016/j.ultsonch.2012.05.004.
[10] O. Baidukova, H. Möhwald, A.S. Mazheika, D.V. Sviridov, T. Palamarciuc, B. Weber, P.V. Cherepanov, D.V. Andreeva, E.V. Skorb, Sonogenerated metal-hydrogen sponges for reactive hard templating, Chem. Commun. 51 (2015) 7606–7609, https://doi.org/10.1039/c4cc10026c.
[11] E. Skorb, D. Shchukin, H. Möhwald, D. Andreeva, Sonochemical design of cerium-rich anticorrosion nanonetwork on metal surface, Langmuir 26 (2010) 16973–16979, https://doi.org/10.1021/la100677d.
[12] E. Kuvyrkov, N. Brezhneva, S.A. Ulasevich, E.V. Skorb, Sonochemical nanostructuring of titanium for regulation of human mesenchymal stem cells behavior for implant development, Ultrason. Sonochem. 52 (2019) 437–445, https://doi.org/10.1016/j.ultsonch.2018.12.024.
[13] J. Dulle, S. Nemeth, E.V. Skorb, T. Irrgang, J. Senker, R. Kempe, A. Fery, D.V. Andreeva, Sonochemical activation of Al/Ni hydrogenation catalyst, Adv. Funct. Mater. 22 (2012) 3128–3135, https://doi.org/10.1002/adfm.201200437.
[14] E.V. Skorb, D. Fix, D.G. Shchukin, H. Möhwald, D.V. Sviridov, R. Mousa, N. Wanderka, J. Schäferhans, N. Pazos-Pérez, A. Fery, D.V. Andreeva, Sonochemical formation of metal sponges, Nanoscale. 3 (2011) 985–993, https://doi.org/10.1039/c0nr00635a.
[15] Y. Zhukova, S.A. Ulasevich, J.W.C. Dunlop, P. Fratzl, H. Möhwald, E.V. Skorb, Ultrasound-driven titanium modification with formation of titania based nanofoam surfaces, Ultrason. Sonochem. 36 (2017) 146–154, https://doi.org/10.1016/j.ultsonch.2016.11.014.
[16] E.V. Skorb, H. Mohwald, D.V. Andreeva, Effect of cavitation bubble collapse on the modification of solids: crystallization aspects, Langmuir 32 (2016) 11072–11085, https://doi.org/10.1021/acs.langmuir.6b02842.
[17] L. Escobar-Alarcón, J.L. Iturbe-García, F. González-Zavala, D.A. Solis-Casados, R. Pérez-Hernández, E. Haro-Poniatowski, Hydrogen production by ultrasound assisted liquid laser ablation of Al, Mg and Al-Mg alloys in water, Appl. Surf. Sci. 478 (2019) 189–196, https://doi.org/10.1016/j.apsusc.2019.01.213.
[18] O. Baidukova, E.V. Skorb, Ultrasound-assisted synthesis of magnesium hydroxide nanoparticles from magnesium, Ultrason. Sonochem. 31 (2016) 423–428, https://doi.org/10.1016/j.ultsonch.2016.01.034.
[19] G. Balducci, L. Bravo Diaz, D.H. Gregory, Recent progress in the synthesis of nanostructured magnesium hydroxide, CrystEngComm 19 (2017) 6067–6084, https://doi.org/10.1039/c7ce01570d.
[20] E.V. Skorb, O. Baidukova, A. Goyal, A. Brotchie, D.V. Andreeva, H. Möhwald, Sononanoengineered magnesium-polypyrrole hybrid capsules with synergetic trigger release, J. Mater. Chem. 22 (2012) 13841–13848, https://doi.org/10.1039/c2jm30768e.
[21] J.R. Ares, F. Leardini, P. Díaz-Chao, J. Bodega, D.W. Koon, I.J. Ferrer, J.F. Fernández, C. Sánchez, Hydrogen desorption in nanocrystalline MgH2 thin films at room temperature, J. Alloy. Compd. 495 (2010) 650–654, https://doi.org/10.1016/j.jallcom.2009.10.110.
[22] J.R. Ares, F. Leardini, P. Díaz-Chao, J. Bodega, J.F. Fernández, I.J. Ferrer, C. Sánchez, Ultrasonic irradiation as a tool to modify the H-desorption from hydrides: MgH2 suspended in decane, Ultrason. Sonochem. 16 (2009) 810–816, https://doi.org/10.1016/j.ultsonch.2009.03.004.
[23] Laboratory of ultrasound technologies and equipment, (n.d.). https://cavitation.bsuir.by/en/, (accessed February 18, 2020).
[24] C.E. Housecroft, A.G. Sharpe, Inorganic Chemistry, Fourth Edition, 2012.
[25] A.N. Kirillov, Vladimir I., Vastrebov, Magnesium alloy for hydrogen production, 5, 494,538, 1996.
[26] J. Rooze, E.V. Rebrov, J.C. Schouten, J.T.F. Keurentjes, Dissolved gas and ultrasonic cavitation – A review, Ultrason. Sonochem. 20 (2013) 1–11, https://doi.org/10.1016/j.ultsonch.2012.04.013.
[27] M. Hauptmann, H. Struyf, P. Mertens, M. Heyns, S. De Gendt, C. Glorieux, S. Brems, Towards an understanding and control of cavitation activity in 1 MHz ultrasound fields, Ultrason. Sonochem. 20 (2013) 77–88, https://doi.org/10.1016/j.ultsonch.2012.05.004.
[28] M. Hauptmann, F. Frederickx, H. Struyf, P. Mertens, M. Heyns, S. De Gendt, C. Glorieux, S. Brems, Enhancement of cavitation activity and particle removal with pulsed high frequency ultrasound and supersaturation, Ultrason. Sonochem. 20 (2013) 69–76, https://doi.org/10.1016/j.ultsonch.2012.04.015.
[29] G. Nithya, B. Thanuja, C.C. Kanagam, Study of intermolecular interactions in binary mixtures of 2′-chloro-4-methoxy-3-nitro benzil in various solvents and at different concentrations by the measurement of acoustic properties, Ultrason. Sonochem. 20 (2013) 265–270, https://doi.org/10.1016/j.ultsonch.2012.05.008.
[30] R. Battino, H.L. Clever, Solubility of Gases in Liquids, Chem. Rev. 66 (1966) 395–463, https://doi.org/10.1002/0470867833.ch3.
[31] J.-H. Ulises-Javier, E. Pardillo-Fontdevila, A. Wilhelm, H. Delmas, Solubility of hydrogen and carbon monoxide in water and some organic solvents, Lat. Am. Appl. Res. 34 (2004) 71–74.
[32] J. Tu, T.J. Matula, A.A. Brayman, L.A. Crum, Inertial cavitation dose produced in ex vivo rabbit ear arteries with optison by 1-MHz pulsed ultrasound, Ultrasound Med. Biol. 32 (2006) 281–288, https://doi.org/10.1016/j.ultrasmedbio.2005.10.001.
[33] N.V. Dezhkunov, A. Francescutto, F. Calligaris, A.V. Kotukhov, Cavitation in pulsed and continuous ultrasound fields, Proc. Int. Sci. Tech. Conf. Dedic. to 50 Anniv. MRTI-BSUIR, 2014, pp. 178–179.
[34] N.V. Dezhkunov, A. Francescutto, P. Ciuti, T.J. Mason, G. Iernetti, A.I. Kulak, Enhancement of sonoluminescence emission from a multibubble cavitation zone, Ultrason. Sonochem. 7 (2000) 19–24 https://doi.org/10.1016/S1350-4177(99)00023-1.
[35] P.L. Marston, Tensile strength and visible ultrasonic cavitation of superfluid 4 He, J. Low Temp. Phys. 25 (1976) 383–407, https://doi.org/10.1007/BF00655838.
[36] W. Lauterborn, C.D. Ohl, The peculiar dynamics of cavitation bubbles, Flow, Turbul. Combust. 58 (1997) 63–76, https://doi.org/10.1007/978-94-011-4986-0_5.
[37] M.P. Brenner, S. Hilgenfeldt, D. Lohse, Single-bubble sonoluminescence, Rev. Mod. Phys. 74 (2002) 425–484, https://doi.org/10.1103/RevModPhys.74.425.
[38] B.-K. Kang, M.-S. Kim, S.-H. Lee, H. Sohn, J.-G. Park, Effect of acoustic cavitation on dissolved gases and their characterization during megasonic cleaning, ECS Trans. 41 (2011) 101–107.
[39] P. Ciuti, N.V. Dezhkunov, G. Iernetti, A.I. Kulak, Cavitation phenomena in pulse modulated ultrasound fields, Ultrasonics 36 (1998) 569–574, https://doi.org/10.1016/S0041-624X(97)00114-5.
[40] R.W. Cargill, The solubility of gases in water-alcohol mixtures, Chem. Soc. Rev. 22 (1993) 135–141, https://doi.org/10.1039/CS9932200135.
[41] A.W. Jones, Determination of liquid/air partition coefficients for dilute solutions of ethanol in water, whole blood, and plasma, J. Anal. Toxicol. 7 (1983) 193–197, https://doi.org/10.1093/jat/7.4.193.
[42] J. Shen, Y. He, J. Wu, C. Gao, K. Keyshar, X. Zhang, Y. Yang, M. Ye, R. Vajtai, J. Lou, P. Ajayan, Liquid phase exfoliation of two-dimensional materials by directly probing and matching surface tension components, Nano Lett. 15 (2015), https://doi.org/10.1021/acs.nanolett.5b01842.
[43] Y. Tomita, M. Tsubota, K. Nagane, N. An-Naka, Behavior of laser-induced cavitation bubbles in liquid nitrogen, J. Appl. Phys. 88 (2000) 5993–6001, https://doi.org/10.1063/1.1320028.
[44] L. Van Wijngaarden, Mechanics of collapsing cavitation bubbles, Ultrason. Sonochem. 29 (2016) 524–527, https://doi.org/10.1016/j.ultsonch.2015.04.006.
[45] S.A. Shchukarev, T.A. Tolmacheva, Solubility of oxygen in ethanol — Water mixtures, J. Struct. Chem. 9 (1968) 16–21, https://doi.org/10.1007/BF00744018.
[46] A. Pal, W. Singh, Speeds of Sound and Viscosities in Aqueous Poly(ethylene glycol) Solutions at 303.15 and 308.15 K, J. Chem.Eng. Data. 42 (1997) 234–237, https://doi.org/10.1021/je960173x.
[47] Azeotropic Data of Ethanol + Cyclohexane from Dortmund Data Bank, (n.d.). http://www.ddbst.com/en/EED/AZD/AZD Ethanol%3BCyclohexane.php.
[48] A. Weissler, Ultrasonic Investigation of Molecular Properties of Liquids. II.1 The Alcohols1a, J. Am. Chem. Soc. 70 (1948) 1634–1640, https://doi.org/10.1021/ja01184a097.
[49] G.G. Miller, J.A. Raleigh, Action of some hydroxyl radical scavengers on radiation-induced haemolysis, Int. J. Radiat Biol. 43 (1983) 411–419, https://doi.org/10.1080/09553008314550471.
[50] C.E. Brennen, Cavitation and Bubble Dynamics, Oxford University Press, New York, 2013, , https://doi.org/10.1017/CBO9781107338760.
[51] S. Skvortsov, Techniques of Ultrasound Cavitation Control, Sci. Educ. Bauman MSTU 15 (2015) 83–100, https://doi.org/10.7463/0215.0759806.
[52] S.D. Lubetkin, Why is it much easier to nucleate gas bubbles than theory predicts? Langmuir 19 (2003) 2575–2587, https://doi.org/10.1021/la0266381 CCC.
[53] M. Ashokkumar, R. Hall, P. Mulvaney, F. Grieser, Sonoluminescence from aqueous alcohol and surfactant solutions, J. Phys. Chem. B 101 (1997) 10845–10850, https://doi.org/10.1021/jp972477b.
[54] C. Liu, E. Bonaccurso, B. Hans-Jürgen, Evaporation of sessile water/ethanol drops in a controlled environment, Phys. Chem. Chem. Phys. 10 (2008) 7150–7157, https://doi.org/10.1039/b808258h.
[55] M. Bobtelsky, The chemical and physical properties of ethanol-water mixtures, J. Chem. Soc. (1950) 3615–3617, https://doi.org/10.1039/JR9500003615.
[56] D.M. Kirpalani, F. Toll, Revealing the physicochemical mechanism for ultrasonic separation of alcohol-water mixtures, J. Chem. Phys. 117 (2002) 3874–3877, https://doi.org/10.1063/1.1495849.
[57] I. Tzanakis, G.S.B. Lebon, D.G. Eskin, K.A. Pericleous, Characterizing the cavitation development and acoustic spectrum in various liquids, Ultrason. Sonochem. 34 (2017) 651–662, https://doi.org/10.1016/j.ultsonch.2016.06.034.
[58] G.J. Price, M. Ashokkumar, F. Grieser, Sonoluminescence Quenching of Organic Compounds in Aqueous Solution : Frequency Effects and Implications for Sonochemistry, J. Am. Chem. Soc. 126 (2004) 2755–2762, https://doi.org/10.1021/ja0389624.
[59] D. Sunartio, F. Grieser, M. Ashokkumar, Sonoluminescence quenching in aqueous solutions of aliphatic diols and glycerol, Ultrason. Sonochem. 16 (2009) 23–27,

https://doi.org/10.1016/j.ultsonch.2008.06.005.
[60] G.A. McFeely, F.R. Somorjai, Studies of the Vaporization, J. Phys. Chem. 76 (1972) 914–918.
[61] P.V. Cherepanov, D.V. Andreeva, Phase structuring in metal alloys: Ultrasound-assisted top-down approach to engineering of nanostructured catalytic materials, Ultrason. Sonochem. 35 (2017) 556–562, https://doi.org/10.1016/J.ULTSONCH.2016.05.006.
[62] A. Kollath, N. Brezhneva, E.V. Skorb, D.V. Andreeva, Microbubbles trigger oscillation of crystal size in solids, Phys. Chem. Chem. Phys. 19 (2017) 6286–6291, https://doi.org/10.1039/c6cp07456a.
[63] P.V. Cherepanov, I. Melnyk, D.V. Andreeva, Effect of high intensity ultrasound on Al3Ni2, Al3Ni crystallite size in binary AlNi (50 wt% of Ni) alloy, Ultrason. Sonochem. 23 (2015) 26–30, https://doi.org/10.1016/j.ultsonch.2014.07.022.
[64] A. Kollath, P.V. Cherepanov, D.V. Andreeva, Controllable manipulation of crystallinity and morphology of aluminium surfaces using high intensity ultrasound, Appl. Acoust. 103 (2016) 190–194, https://doi.org/10.1016/j.apacoust.2015.06.016.
[65] P.V. Cherepanov, M. Ashokkumar, D.V. Andreeva, Ultrasound assisted formation of Al-Ni electrocatalyst for hydrogen evolution, Ultrason. Sonochem. 23 (2015) 142–147, https://doi.org/10.1016/j.ultsonch.2014.10.012.